Progress In Electromagnetics Research B, Vol. 81, 45–61, 2018

AC Induced Corrosion Assessment of Buried Pipelines near HVTLs: A Case Study of South Africa

Kazeem B. Adedeji[1, *], Akinlolu A. Ponnle[2], Bolanle T. Abe[1], Adisa A. Jimoh[1], Adnan M. Abu-Mahfouz[1, 3], and Yskandar Hamam[1, 4]

Abstract—Metallic pipelines have attendant problems of alternating current (AC) assisted corrosion when installed in the utility corridor with high voltage transmission lines. Research studies in the past and recent years have shown that this corrosion is a primary function of the AC density through the pipe coating defect. While several other AC corrosion risk assessment indices have been proposed, the AC density is regarded as a valuable parameter in assessing pipeline corrosion risk due to AC interference. Also, there exists a threshold value which, if exceeded, guarantees the possibility of pipeline corrosion damage. However, for buried pipelines, monitoring these AC corrosion assessment indices is a major challenge. Therefore, to avoid severe corrosion damage to such pipelines, a corrosion assessment for evaluating the corrosion risk of the pipelines due to AC interference is presented in this paper. The assessment was demonstrated on a buried pipeline in one of the Rand Water sites, South Africa where AC interference is frequent. The overall simulation results yield useful information which may be essential for pipeline operators, most especially Rand Water, South Africa and corrosion engineers for AC corrosion assessment of metallic pipelines installed near transmission lines. The analysis presented in this paper may also be used for the evaluation of a safe position for installing new pipelines near existing power lines right-of-way.

1. INTRODUCTION

Alternating current assisted corrosion poses a threat to the integrity of pipelines and has been a subject of research within the pipeline research community and corrosion engineers. This is due to the frequent installation of pipelines in the right-of-way (ROW) of high voltage transmission lines (HVTLs). Water or gas transporting pipelines in the shared corridor have attendant problems of induced voltage due to the time varying magnetic field produced by the transmission line current. The induced voltage depends, among other factors, on the transmission line configuration, line current and soil resistivity [1–3]. This causes current circulation between the pipeline and the surrounding soil through a coating defect on the pipe. At the defect point, an anodic reaction takes place, resulting in the dissolution of the metal [5] as illustrated in Equation (1).

$$M \rightarrow M^{n+} + ne^{-} \tag{1}$$

Considering Equation (1), the metal is attacked through the migration of ions away from its surface resulting in metal loss which is visible over time as corrosion [4]. This is usually regraded as AC assisted corrosion [4–7]. With the pipeline coating defect ranging from a few millimetres to several decimeters, previous research works [8–10] revealed that the highest corrosion activities occur on pipeline with smaller defects.

Received 5 April 2018, Accepted 28 May 2018, Scheduled 13 June 2018

* Corresponding author: Kazeem Bolade Adedeji (adedejikb@tut.ac.za).

[1] Department of Electrical Engineering, Tshwane University of Technology, Pretoria, South Africa. [2] Department of Electrical and Electronics Engineering, Federal University of Technology, Akure, Ondo State, Nigeria. [3] Meraka Institute, CSIR, Pretoria, South Africa. [4] ESIEE-Paris, France.

1.1. AC Interference from HVTLs on Metallic Pipelines

The interference on pipelines from nearby HVTLs may be as a result of inductive, conductive and capacitive coupling from the transmission line [1–3, 11]. The inductive coupling affects both aerial and underground pipelines that run parallel to or in the vicinity of HVTL. In this coupling, a voltage is induced into the pipelines due to the time varying magnetic fields produced by the transmission line currents. The capacitive coupling only affects structures located above the ground [11, 12]. For underground pipeline, the effect of capacitive coupling may be neglected due to the screening effect of the earth against electric fields. The resistive coupling between a HVTL and a metallic pipeline is only relevant during ground faults where significant magnitude of current flows into the ground [11, 12]. Irrespective of the type of coupling from the transmission line, this interference varies with the electrical characteristics and geometry of the individual system [13]. The relevance of this interference is crucial to the safety of operational personnel and for the protection of buried metallic structures from corrosion. To this objective, the National Association of Corrosion Engineers (NACE) imposes a voltage limit of 15 Vr·m·s under normal operating condition of the transmission line, for safety of personnel working on the pipeline [14]. In the past, AC mitigation systems have been proposed to mitigate the effect of AC potentials on metallic pipelines. Among others, the use of AC decoupling devices, zinc ribbon, ground mats and Faraday cage have some level of success. Even with the use of these systems, several cases of AC interference assisted corrosion have been reported.

Furthermore, in an effort to protect metallic pipelines from AC corrosion with the application of cathodic protection (CP) system, the presence of AC interference adversely affects the performance of the CP system. The interference caused by AC from the transmission lines shifts the CP potential applied on pipelines from the design value of −0.85 V stipulated by the European Technical Specification EN12954 [15]. The subject is being studied extensively in the past and recent years and has becomes a subject of discussion at numerous congresses organized by scientific organizations [16–18] in the past years. Also, previous research works have shown that the corrosion risk due to AC interference relates to pipeline isolated defect and the current density through such defect [17–19].

There is consensus among authors on the AC density as a primary factor in determining corrosion rate in the presence of AC interference. After several research efforts, the following conclusions were made:

(i) For pipelines having an AC density of 30 A/m^2 through its coating defect, there is probably no risk of accelerated corrosion.

(ii) For AC density between 30 A/m^2 and 100 A/m^2, corrosion is possible.

(iii) For AC density greater than 100 A/m^2, corrosion damage is expected.

Some other pipeline AC corrosion assessment indices reported in the literature include the pipe-to-soil potential [20] and the relative risk (RR) value of AC corrosion along the length of the pipe [21]. These research works revealed that in order to reduce the corrosion likelihood on pipelines due to the inductive effects from HVTLs, the measured or estimated pipe-to-soil potential on these pipelines should at any time, not exceed:

(i) 10 V where the soil resistivity is greater than 25 Ω·m; and

(ii) 4 V where the soil resistivity is less than 25 Ω·m.

The RR index proposed by Philip [21] for assessing the corrosion risk of pipelines due to AC interference is based on the historical pattern of AC corrosion cases which revealed that the corrosion risk occurs due to higher voltage and lower soil resistivity. As a result of this findings, the RR index may be defined as

$$RR = \frac{V_{ac}}{\rho_s} \tag{2}$$

where V_{ac} is the pipe-to-soil potential along the length of the pipe, and ρ_s is the resistivity of the surrounding soil in which the pipe is buried. Philip [21] indicated that for RR value greater than 0.22, the AC density in such location should be monitored and additional AC mitigation system may be installed.

It is evident that the induced potential on pipelines due to the coupling effect from the transmission line is the primary cause of AC assisted corrosion on pipelines and crucial to evaluating the AC corrosion

assessment indices. In the past and recent years, several computational methodologies have been proposed to estimate the induced potential on metallic pipelines. These include the use of circuit analysis method [22, 23] or numerical methods using finite element approach [11, 24–26]. The circuit analysis approach involves the computation of mutual impedance between two circuits (for instance, power line conductors to metallic pipelines). In this approach, each phase conductor of the line induces a voltage on the metallic pipeline through its corresponding mutual impedance. Several mutual impedance approximations are reported in the literature. Among the notable approximations include the Carson-Clem approximation, Pollaczek integral [27] and its analytical approximation [28], Lucca and Ametani mutual impedance approximations [27–31]. Among these approximations, the Carson-Clem approximation is widely adopted.

The level of the induced potential together with the other AC corrosion assessment indices may be evaluated and monitored at any time, for onward application of AC mitigation strategies in locations where the indices tend to exceed the threshold. Rand Water, South Africa is experiencing corrosion of the installed pipelines due to the shared corridor with high voltage transmission lines. In order to avoid severe corrosion damage to such pipelines, a corrosion assessment for evaluating the corrosion risk of the pipelines due to AC interference is presented in this paper. The assessment was carried out on a buried pipeline using a real-life interference problem in one of the Rand Water sites in South Africa where AC interference is frequent. The rest of the paper is organised as follows. Section 2 presents the methods used for the assessment featuring the estimation of the AC corrosion risk assessment indices. In Section 3, the results of the AC corrosion assessment using an interference problem in a location in South Africa are presented while Section 4 concludes the paper and provides the future work.

2. RESEARCH METHODS

This work focuses on assessing the AC corrosion risk on a buried pipeline accomplished by evaluating the AC assisted corrosion indices on the pipe due to the inductive coupling effect from four overhead HVTLs at Strydpan, South Africa.

2.1. Network of the HVTL and Pipeline Description

Figure 1 illustrates the schematic diagram of the transmission lines and pipeline model ROW. As may be seen in Figure 1, the system consists of four single circuit 275 kV HVTLs in a horizontal configuration (with two overhead earth wires on each tower) and a water pipeline buried at a depth h_p beneath the soil surface. The pipeline which has a radius r_p is coated with polyethylene polymer with a coating thickness t_c and runs parallel to the HVTLs for a length L. The transmission lines tower dimension and configurations are depicted in Figure 1. The transmission lines were evenly spaced at a tower centre to centre distance of 32 m from each other.

Under steady state condition of the transmission line, the longitudinal induced voltage on the pipe may be estimated using Carson's methodology [27]. The methodology is based on evaluating the mutual impedances between the line conductors and the pipeline. It is worthwhile to mention that for the sake of simplicity without any noticeable technical error, the soil is assumed to be homogenous with uniform soil resistivity. Also, the reciprocal effects of the earth wires on each other are neglected.

2.2. Induced AC Voltage Analysis

Consider a single-circuit overhead line with k^{th} earth wire, each current in the phase conductors induces a voltage on the pipeline through the appropriate mutual impedance between the pipeline and the conductor. The longitudinal electromotive force (LEF) E_p induced on the pipeline due to the three-phase currents I_R, I_W, I_B and the earth wire current may be expressed as

$$E_p = I_R Z_{Rp} + I_W Z_{Bp} + I_B Z_{Bp} - \sum_{k=1}^{n} I_{g_k} Z_{g_k p} \tag{3}$$

where I_R, I_W, I_B and I_{gk} are the steady state currents in the phase conductors and the k^{th} earth wires; Z_{Rp}, Z_{Wp}, Z_{Bp}, Z_{gkp} are the mutual impedances (Ω/m) between the phase conductors, the k^{th} earth

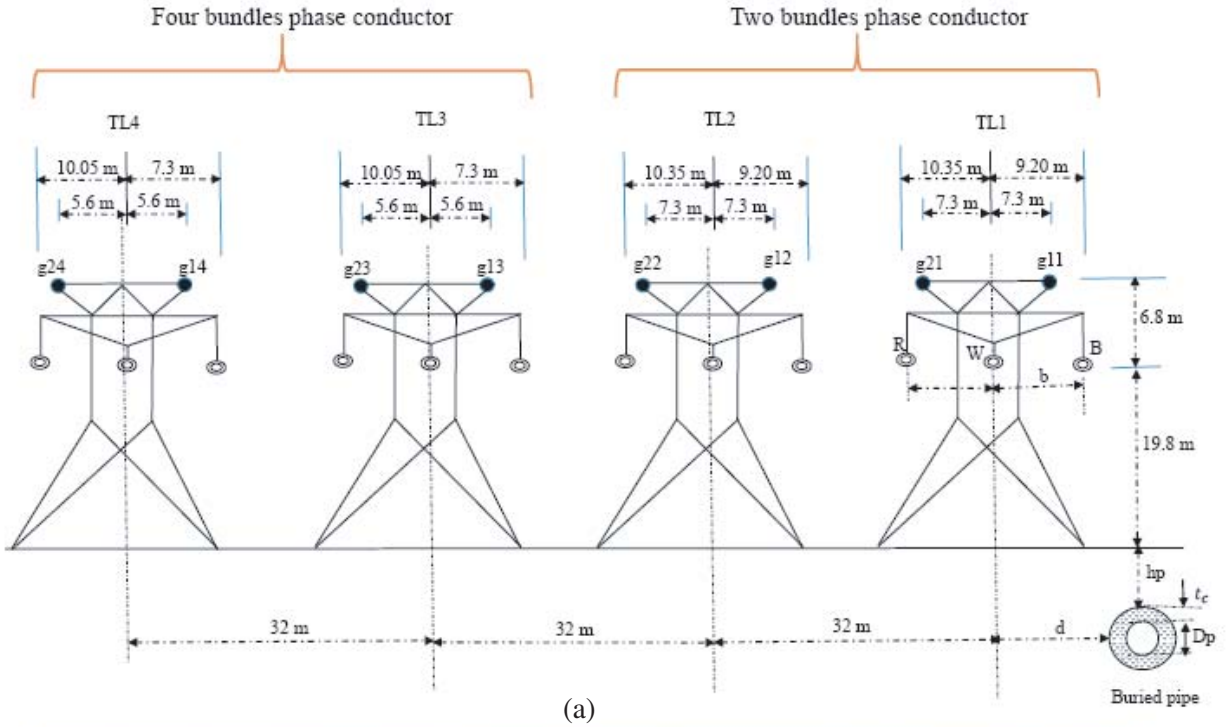

(a)

(b)

Figure 1. The HVTL and pipeline model at Strydpan site (a) schematic diagram (b) snapshot.

wire and the pipeline; n represents the number of earth wires on the tower. The potential drop across the k^{th} earth wire due to the effect of the phase conductors is expressed as

$$V_{g_k} = I_R Z_{Rg_k} + I_W Z_{Wg_k} + I_B Z_{Bg_k} \tag{4}$$

Therefore, the currents in the earth wires I_{gk} may be expressed as

$$I_{g_k} = \frac{V_{g_k}}{Z_{gg_k}} = \frac{1}{Z_{gg_k}} \left(I_R Z_{Rg_k} + I_W Z_{Wg_k} + I_B Z_{Bg_k} \right) \tag{5}$$

where Z_{ggk} denotes the self-impedance of the k^{th} earth wire. Substituting Eq. (5) into Eq. (3) and by further simplification, the longitudinal EMF induced on the pipeline due to the coupling effect of the i^{th} transmission line may be expressed as

$$E_{p_i} = I_{R_i} \left(Z_{R_i p} - \sum_{k=1}^{n} \frac{Z_{R_i g_k} Z_{g_k p}}{Z_{gg_k}} \right) + I_{W_i} \left(Z_{W_i p} - \sum_{i=1}^{n} \frac{Z_{W_i g_k} Z_{g_k p}}{Z_{gg_k}} \right) + I_{B_i} \left(Z_{B_i p} - \sum_{k=1}^{n} \frac{Z_{B_i g_k} Z_{g_k p}}{Z_{gg_k}} \right) \tag{6}$$

In Eq. (6), i is an integer ranging from $1, 2, \ldots, N$. N represents the number of transmission line ($N = 4$ for this study). Also, I_{Ri}, I_{wi} and I_{Bi} are the steady state current in the phase conductors of

the i^{th} transmission line, and Z_{Ri}, Z_{Wi} and Z_{Bi} are the mutual impedances between the R-W-B phase conductors of the i^{th} transmission line and the pipeline. It should be noted that the steady state current in each of the phase conductors (I_{Ri}, I_{wi} and I_{Bi}) is alternating with a phase angle of 120°, 0, −120° to each other as

$$\left.\begin{array}{l} I_{Ri} = |I_{Ri}|\,(\cos 120 + j \sin 120) \\ I_{Wi} = |I_{Wi}| \\ I_{Bi} = |I_{Bi}|\,(\cos 120 - j \sin 120) \end{array}\right\} \tag{7}$$

The mutual impedance between two circuits with earth return, say a pipeline p and an overhead transmission line phase conductor R, W, B or earth wire conductor g, or between the earth wire and the phase conductors may be evaluated using Eq. (8) as

$$Z_{p-m} = \frac{\mu_0 \omega}{8} + j\left(\frac{\mu_0 \omega}{2\pi} \log_e\left(\frac{\delta_e}{D_{p-m}}\right)\right) \quad \forall m \in (R_i, W_i, B_i, g_{k-i}) \tag{8}$$

where μ_0 denotes the magnetic permeability of free space, ω the angular frequency of operation of the transmission line, and δ_e the depth of equivalent earth return. Also, D_{p-m} is the geometric mean distances (GMDs) linking each of the R-W-B or g_k conductors and the pipeline or between the R-W-B phase conductors and the k^{th} earth wire. The self-impedance of the earth wire conductors with earth return may be expressed as

$$Z_{gg_k} = R_{g_k} + \frac{\mu_0 \omega}{8} + j\left(\frac{\mu_0 \omega}{2\pi}\left[\frac{1}{4} + \log_e\left(\frac{\delta_e}{R_{GM_k}}\right)\right]\right) \tag{9}$$

In Eq. (9), R_{gk} is the AC resistance of the k^{th} earth wire, and R_{GMk} is the geometric mean radius of the k^{th} earth wire conductors. The depth of equivalent earth return is a function of the soil resistivity ρ_{soil} and the transmission line operating frequency f. This may be evaluated as

$$\delta_e = 658.87\sqrt{\frac{\rho_{\text{soil}}}{f}} \tag{10}$$

The D_{p-m} in Eq. (8) may be computed by applying Pythagoras theorem to the transmission line/pipeline coordinates shown in Figure 2 as

$$D_{p-m} = \left((x_p - x_m)^2 + (y_m - y_p)^2\right)^{1/2} \quad \forall m \in (R_i, W_i, B_i, g_{k-i}) \tag{11}$$

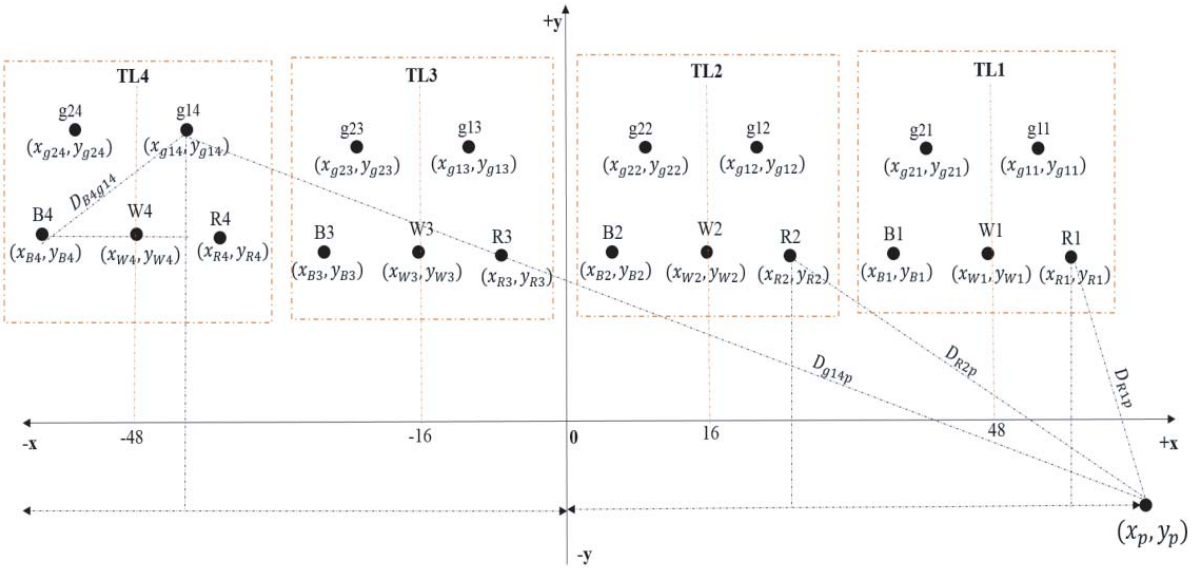

Figure 2. Coordinates of the HVTL-pipeline ROW for the study site.

where x_p represents the horizontal position of the pipeline across the transmission line ROW, and $y_p = (h_p + r_p + t_c)$ represents the pipe depth from the ground to the centre of the pipe. It should be noted that $y_m \, \forall m \in (R_i, W_i, B_i, g_{k-i})$ represents the various heights of the phase conductors or the earth wire from the ground surface while their horizontal position may be represented by $x_m \, \forall k \in (R_i, W_i, B_i, g_{k-i})$ on the x-coordinate.

The longitudinal induced EMF (V/m) on the pipeline is the resultant of the individual inductive coupling effects of the N transmission lines which may be computed as

$$E_p = \sum_{i=1}^{N=4} E_{p_i} \tag{12}$$

Therefore, the longitudinal induced voltage (V) on the entire pipeline exposure length L may be computed as

$$V_p = E_p L \tag{13}$$

2.3. Evaluation of the Pipe-to-soil Potential

A pipeline under an inductive coupling from the transmission line may be viewed as a lossy transmission line having a series impedance and a shunt admittance together with a distributed voltage source. The voltage source is equivalent to the longitudinal induced EMF on the pipeline. The equivalent circuit diagram of a distributed pipeline section of length L in parallel with an overhead HVTL is shown in Figure 3. In this figure, the pipeline has a termination impedance of Z_1 and Z_2 seen from ends A and B.

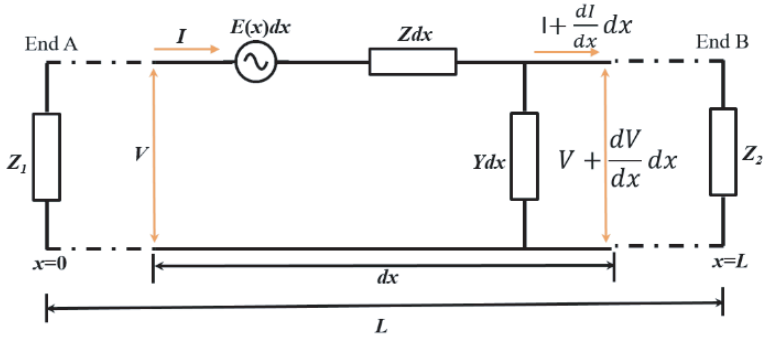

Figure 3. An equivalent circuit of a buried metallic pipeline due to coupling from an overhead transmission line.

Considering Figure 3, each pipeline incremental length dx may be described by its source voltage $E(x)dx$ where $E(x)$ represents the longitudinal induced EMF on the pipe, estimated in Subsection 2.2. Z and Y denote the pipeline impedance and shunt admittance per unit length, respectively. The distributed voltage and current along the pipeline incremental length may be obtained by solving the well-known transmission lines differential equations relating the quantities E, V and I as

$$\frac{d}{dx} V(x) = E(x) - ZI(x) \tag{14}$$

$$\frac{d}{dx} I(x) = -YV(x) \tag{15}$$

Differentiating Eq. (14) with respect to x and substituting Eq. (15) into the resulting expression, one may write

$$\frac{d^2}{dx^2} V(x) = ZYV(x) + \frac{d}{dx} E(x) \tag{16}$$

$$\frac{d^2}{dx^2} V(x) = \gamma^2 V(x) + \frac{d}{dx} E(x) \tag{17}$$

From Eq. (17), $\gamma = \sqrt{ZY}$ represents the pipeline propagation constant (m^{-1}).

It should be noted that the longitudinal induced EMF is constant under both steady state and fault conditions along the entire exposure length of the pipeline. This means that $E(x) = E_p$. Resolving the expressions represented by Eq. (17), the pipe-to-soil potential $V(x)$ along the pipeline section at any point x between zero and L may be estimated as

$$V(x) = \frac{E_p}{\gamma}\left\{\frac{\left[Z_2(Z_1-Z_0)-Z_1(Z_2+Z_0)e^{\gamma L}\right]e^{-\gamma x}-\left[Z_1(Z_2-Z_0)-Z_2(Z_1+Z_0)e^{\gamma L}\right]e^{-\gamma(L-x)}}{(Z_1+Z_0)(Z_2+Z_0)e^{\gamma L}-(Z_1-Z_0)(Z_2-Z_0)e^{-\gamma L}}\right\} \quad (18)$$

From Eq. (18), $Z_0 = \sqrt{Z/Y}$ denotes the pipeline characteristics impedance (Ω).

For a pipe section which continues for some kilometres beyond ends A and B, the termination impedances Z_1 and Z_2 may be taken as equal to the pipeline characteristics impedance seen from points A and B, that is, $Z_1 = Z_2 = Z_0$. Applying this hypothesis to the expressions in Eq. (18), the pipe-to-soil potential may be expressed as

$$V(x) = \frac{E_p}{2\gamma}\left[e^{-\gamma(L-x)} - e^{-\gamma x}\right] \quad (19)$$

For a buried coated pipeline, the longitudinal impedance Z and its shunt admittance Y per unit length may be expressed using Eqs. (20) and (21) [32]

$$Z = \frac{1}{\pi D_p}\sqrt{\pi f \rho_p \mu_0 \mu_p} + \frac{\pi f \mu_0}{4} + j\left[\frac{1}{\pi D_p}\sqrt{\pi f \rho_p \mu_0 \mu_p} + \mu_0 f \ln\left(\frac{3.7}{D_p}\sqrt{\frac{\rho_{\text{soil}}}{2\pi f \mu_0}}\right)\right] \quad (20)$$

$$Y = \frac{\pi D_p}{\rho_c t_c} + j\left(2\pi f \frac{\varepsilon_0 \varepsilon_c \pi D_p}{t_c}\right) \quad (21)$$

In Equations (20) and (21), D_p denotes the pipeline diameter, ρ_p the resistivity of the pipeline, μ_0 the permeability of free space given as $4\pi \times 10^{-7}$ H/m, and μ_p the relative permeability of the pipeline. Also, ρ_c represents the resistivity of the pipe coating material, ε_c the relative permittivity of the pipe coating material, and ε_0 the permittivity of free space expressed as 8.85×10^{-12} F/m.

2.4. Evaluation of the AC Density through a Coating Defect

The alternating current (AC) flowing out of the pipe through a coating defect of a surface area results in an AC density at the point of defect as illustrated in Figure 4.

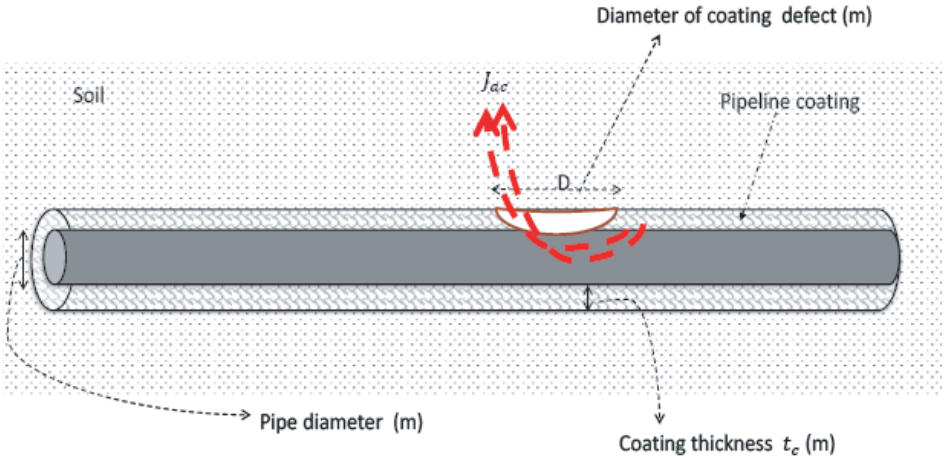

Figure 4. Illustration of current density through a pipeline coating defect.

At the point of defect, the pipe has a resistance R to remote earth which may be expressed as

$$R = \frac{\rho_{\text{soil}}}{2D}\left(1 + \frac{8t_c}{D}\right) \quad (22)$$

where D represents the diameter of the defect. Substituting Eq. (22) into the traditional ohm's law expression, one may write

$$I = \frac{V}{\frac{\rho_{\text{soil}}}{2D}\left(1 + \frac{8t_c}{D}\right)} = \frac{2D^2 \times V_{ps}}{\rho_{\text{soil}}\left(D + 8t_c\right)}$$

Assuming a defect of circular geometry with surface area $A = \pi D^2/4$, the current density J through the defect may well be expressed as $J = I/A$. By further substitution, the AC density J_{ac} (A/m^2), through a coating defect at a point x along the length of the pipeline section may be expressed as

$$J_{ac}\left(x\right) = \frac{8V\left(x\right)}{\pi\rho_{\text{soil}}\left(D + 8t_c\right)} \tag{23}$$

where $V(x)$ represents the pipeline-to-soil potential at a point$x$, along the length of the pipeline section estimated earlier in Subsection 2.3.

2.5. The Relative Risk Value of AC Corrosion Derivation

The relative risk (RR) value of AC corrosion at any point x along the length of the pipeline buried in a soil may be expressed as

$$RR\left(x\right) = \frac{V\left(x\right)}{\rho_{\text{soil}}} \tag{24}$$

2.6. Case Study Parameters Used for Simulation

To carry out the AC corrosion risk assessment of the pipeline in the study site, the data relevant to the layout illustrated in Figure 1 was used. These data include the parameters of the pipe, the soil and the transmission lines in the study site as illustrated in Table 1 to Table 3. Also, the effect of the phase conductor transpositions of the transmission lines in the study site on the AC corrosion risk assessment indices is also considered. For the layout in Figure 1, the phase conductor transposition has the following options:

(i) TL1-TL2 phase conductors are un-transposed; TL3-TL4 phase conductors un-transposed:
(ii) TL1-TL2 phase conductors are un-transposed; TL3-TL4 phase conductors transposed:
(iii) TL1-TL2 phase conductors are transposed; TL3-TL4 phase conductors un-transposed:
(iv) TL1-TL2 phase conductors are transposed; TL3-TL4 phase conductors transposed.

Table 1. The pipe parameters.

S/N	Parameter	Value
1	Pipe material	Steel
2	Diameter	1000 mm
3	Burial depth	1 m
4	Defect size (diameter)	1 mm
5	Exposure length	1000 m
6	Resistivity of steel pipeline	0.17×10^{-6} Ω·m
7	Relative permeability of the pipe metal	300
Pipeline Coating		
9	Coating type	Polyethylene
10	Coating thickness	4 mm
11	Resistivity of the pipe coating material	20×10^{6} Ω·m
13	Relative permittivity of the pipe coating	2.3

Table 2. The soil parameters.

S/N	Parameter	Value
1	Measured resistivity	12.96 Ω·m
2	Relative permeability	1

Table 3. The transmission line parameters.

S/N	Parameter	Value
1	Operating frequency	50 Hz
2	Operating voltage	275 kV
3	Phase conductor type	Zebra
4	Peak load current per conductor	410 A
Overhead earth wire parameters		
4	Type	19/2.65 mm galvanized steel wire
5	Diameter	13.48 mm
5	AC resistance	3.44×10^{-3} Ω/m

3. RESULTS AND DISCUSSION

3.1. Induced Voltage Analysis for Pipeline Placement in the Transmission Line ROW

The induced voltage on the buried pipeline due to the inductive coupling effect from the transmission lines was computed under normal operating condition of the transmission line. The evaluation was based on different phase conductor transpositions of the transmission lines in the study site. Figure 5 shows the profile of the induced voltage on the pipeline due to the inductive coupling effect of the four

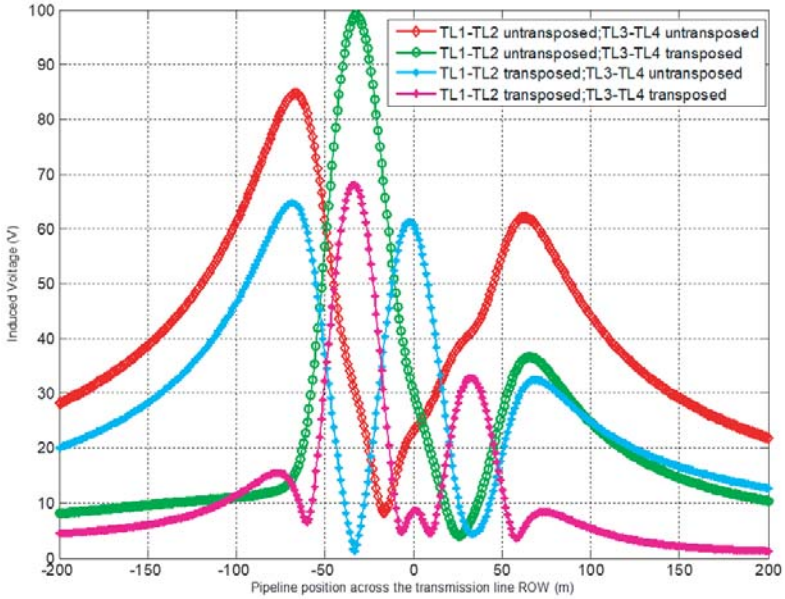

Figure 5. Longitudinal induced voltage on the pipeline due to the various transmission line phase conductor arrangements.

HVTLs, with the variation in the position of the pipeline across the transmission line ROW.

The effect of the transmission lines phase conductor arrangement is depicted by the figure. Considering the option (i) of the phase conductor transposition. This indicates that the phase conductors of the transmission lines are arranged in the form "RWB-RWB; RWB-RWB". From this, it may be observed that the maximum voltage occurs on the pipe at some distance beyond the last phase conductors of the two extreme ends of the transmission lines. These two ends of the transmission lines (Figure 2) corresponds to 57.2 m for the last phase conductor of TL1 and −58.05 m for that of TL4 in Figure 5. Moreover, the Eskom guide for installing structures near a transmission line servitude in South Africa stated that no structure is permitted for a distance of 23.5 m for 275 kV transmission line measured from the centre line of the transmission line [33]. However, the two extreme transmission lines have a centre line distance of 48 m and −48 m measured from the reference point as shown in Figure 2. Therefore, using the Eskom requirement of placing structures, these points corresponds to a distance of 71.5 m for (TL1) and −71.5 m (for TL4) on Figure 5. Looking at these two points, it may be observed that for new pipeline installations along the transmission lines, pipelines installed near TL1, and away from this point (71.5 m) will experience lower induced voltage compared to those installed near TL4. Thus, to reduce the induced voltage on pipelines, when considering the option (i) of the phase conductor transposition, the pipelines should be installed beside TL1 and with a minimum distance of 14.3 m from its last phase conductor. Furthermore, considering the option (ii) of the phase conductor transposition (RWB-RWB; BWR-BWR), it may be observed that there is a large reduction in voltage, especially on the other side of the transmission lines (TL4). It is obvious from the figure that pipelines installed near TL1 for these allowable distances (71.5 m away the centre line of the transmission lines) will experience much higher induced voltage than those installed near TL4.

Moreover, in the option (iii) of the phase conductor transposition, it is obvious that pipelines installed near TL1 for the same allowable distances will experience much lower induced voltage with a relatively wide margin, than those installed near TL4. The effect of choosing the option (iv) of the phase conductor transposition on the voltage induced on the pipe is also analysed. In line with the results presented for the effect of choosing first and third options, it is obvious that pipelines installed near TL1 for the same allowable distances will experience a relatively lower induced voltage than those installed near TL4.

In general, the above analyses indicate that a pipeline installed near TL1 has a relatively low induced voltage in three out of the four phase transposition options. One may conclude that for Rand Water new pipeline installations in this site, the pipelines should be installed near TL1, and at a safe distance from its last phase conductors. With this, the induced voltage on the pipeline in the ROW of the transmission lines will significantly reduce. Furthermore, the transmission line with TL1-TL2; TL3-TL4 phase conductors un-transposed has the profound inductive effect on the pipeline. However, with a direct transposition of the transmission line phase conductors (option (iv)), there is a large reduction in the induced voltage on the pipeline. This indicated that the inductive coupling effect on pipelines installed near a transmission line with a phase conductor's transposition of this type is minimal.

3.2. Pipe-to-Soil Potential, AC Density and Relative Risk of AC Corrosion Computation

In this section, the computed pipe-to-soil potential, relative risk value of AC corrosion and AC density at a point 100 m on the pipeline due to the four options for the transmission line phase conductors' transposition is shown in Figure 6 to Figure 8. Analysing Figure 6, it may be observed that pipeline installed near TL1 has the lowest pipe-to-soil potential, the least occurs for option (iv) of the phase conductor transposition. Furthermore, similar pattern is noticed for the relative risk value of AC corrosion plot (Figure 7) and the AC density plot (Figure 8). In each case, pipeline installed near TL1 experiences the least relative risk value of AC corrosion and the AC density through the 1 mm defect at a point 100 m on the pipeline.

3.3. Effect of the Transmission Line Steady State Current on the AC Density and Pipeline Corrosion Rate

Due to increase in energy demand, Figure 9 concerns the effect of increasing transmission line steady state current on the AC density (a major index of AC corrosion), through four different coating defects

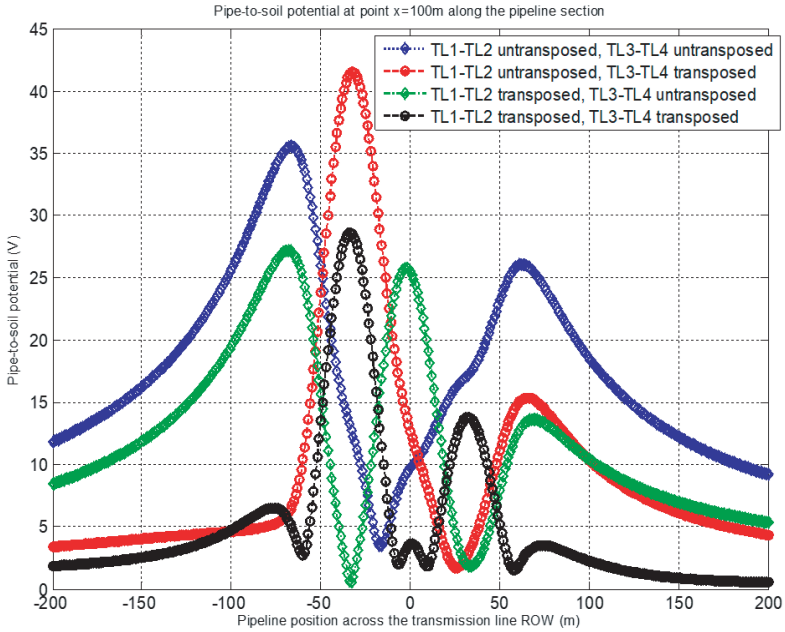

Figure 6. Pipe-to-soil potentials at 100 m with pipeline variations across the transmission lines due to various phase conductor transpositions.

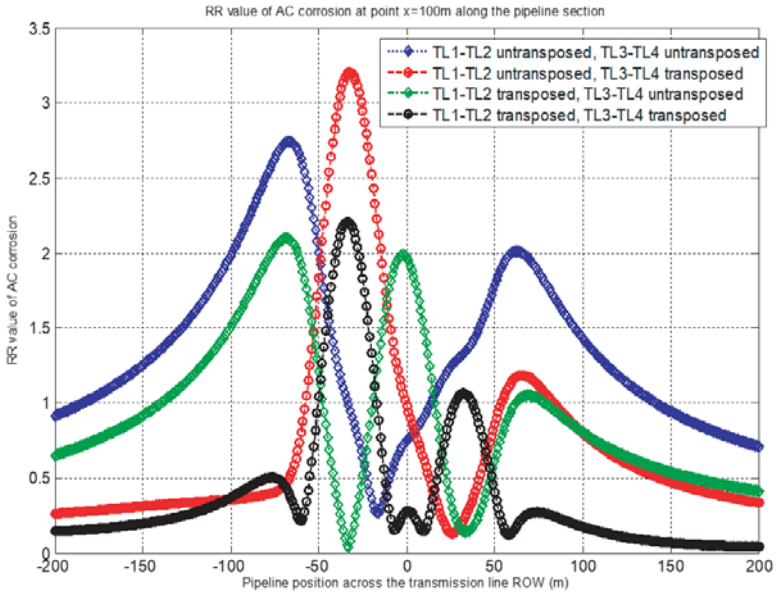

Figure 7. The relative risk of AC corrosion at 100 m with pipeline variations across the transmission lines due to various phase conductor transpositions.

of varying sizes at a point 100 m on the pipe. For this analysis, the first option for the phase conductors' transposition was selected. In addition, the pipeline position at a distance of 80 m (near TL1) away from the transmission line right-of-way (according to the Eskom guide discussed earlier) was considered.

Considering the figure, it may be observed that there is a linear relationship between the transmission line steady state current and the AC density. The AC density increases with increasing transmission line current. The result further revealed that higher AC corrosion activities (high AC density) occur on the pipeline with smaller defect sizes while the least corrosion activities occur on large

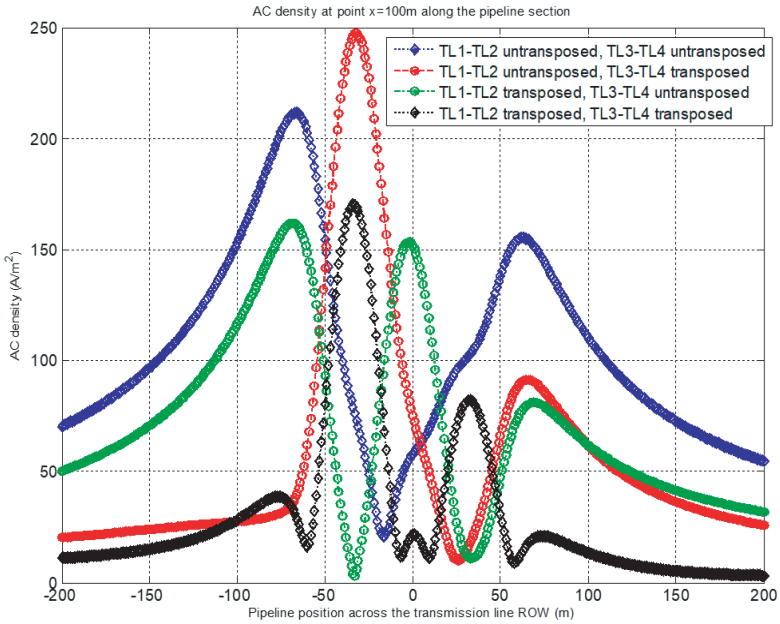

Figure 8. The AC density through a 1 mm defect at 100 m on the pipeline with pipeline variations across the transmission lines due to various phase conductor transpositions.

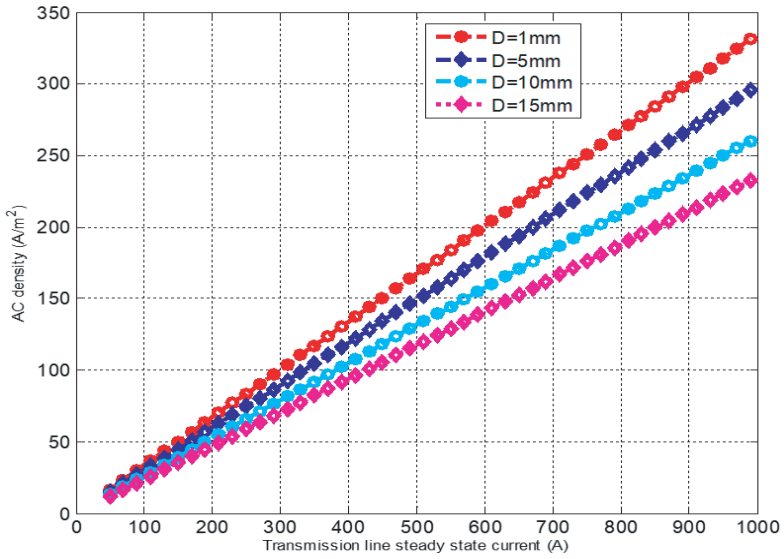

Figure 9. Variation of the AC density with transmission line current for different sizes of coating defect.

defect sizes. Judging from the research works in [34, 35] in which AC density is a linear function of the corrosion rate, one may safely conclude that the corrosion rate increases with increasing transmission line current. Therefore, by studying the historical data of the variations in the transmission line current, the corrosion penetration rate of pipeline installed in such site may be predicted.

3.4. Effect of Soil Resistivity on the AC Density and Pipeline Corrosion Rate

To assess the level of the threat of corrosion to metallic pipelines, the soil resistivity of the surrounding environment cannot be overlooked. Figure 10 relays the effect of the soil resistivity variations on the

AC density through different coating defects on the pipeline. The same condition as in Section 3.3 for placing the pipeline, and the AC density through the different defects at a point 100 m on the pipeline is also considered herein. It may be observed that the AC density through defects (1 mm, 5 mm, 10 mm, and 15 mm) decreases with increasing soil resistivity. For the measured soil resistivity of 12.96 Ω·m, the AC density through a 1 mm defect (see Figure 10), is above 160 A/m^2. This value exceeds the threshold value of AC density which guarantees a higher likelihood of corrosion damage to the pipeline.

Furthermore, considering the changes in the value of AC density with the variations in the soil resistivity as illustrated in Figure 10, there is a large reduction in AC density for soil resistivity between 10 Ω·m to 20 Ω·m with a wider margin. However, with increased soil resistivity from 20 Ω·m to 30 Ω·m and more, a little reduction in the value of the AC density may be observed. Also, this is almost constant, though at a reduced magnitude for higher values of soil resistivity. The result indicated that

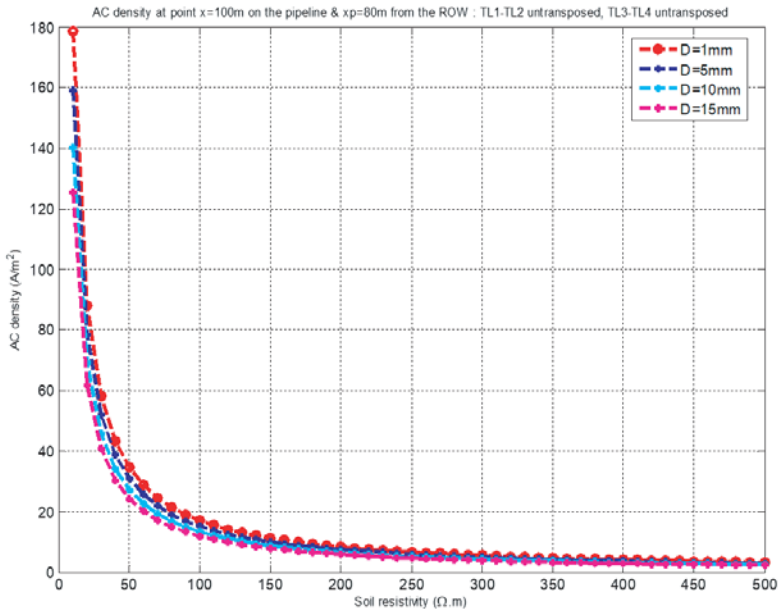

Figure 10. Variation of the AC density with soil resistivity for different sizes of coating defect.

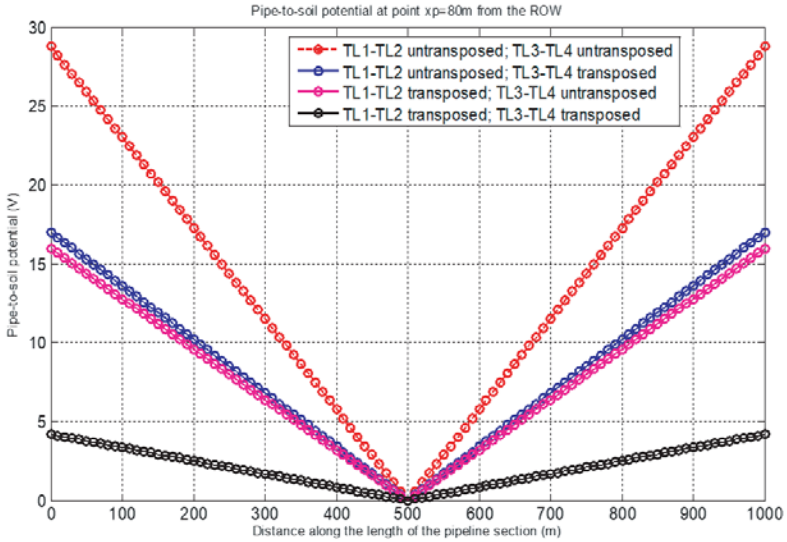

Figure 11. Pipe-to-soil potential along the length of the pipeline.

the lower the soil resistivity, the higher the tendency of increased corrosion at the pipe coating defects. Hence, more attention should be given to pipelines, if at any time, the measured soil resistivity in such environment is relatively low.

3.5. Computed Pipe-to-Soil Potential, Relative Risk of AC Corrosion and the AC Density along the Pipeline Length Section

In the previous sections, the analysis of the corrosion assessment indices was conducted at a point 100 m on the pipeline. In this section, the computations of these indices at different points along the length of the pipeline parallel section is analysed. These are presented in Figure 11 to Figure 13. The pipeline

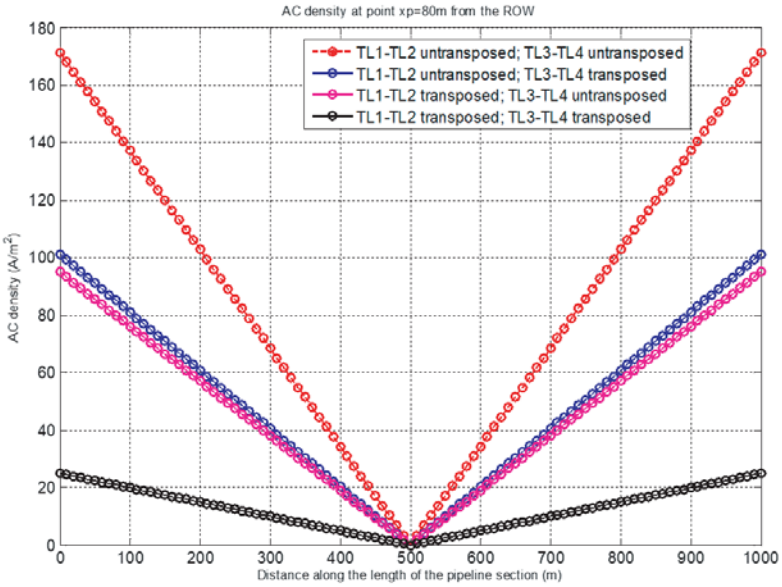

Figure 12. AC density through a 1 mm defect along the length of the pipeline.

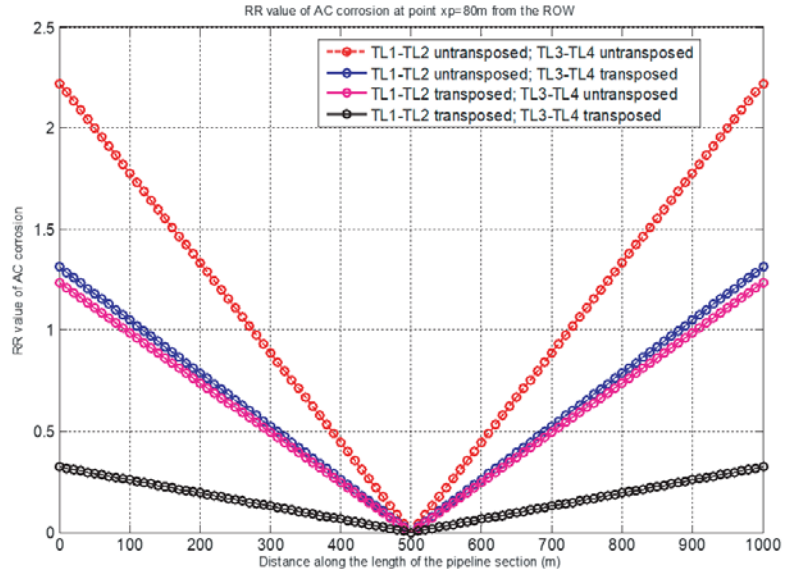

Figure 13. Relative risk of AC corrosion along the length of the pipeline.

is positioned at a distance of 80 m from the transmission lines ROW. The analysis was also considered for the four options of the transmission line phase conductors' transpositions.

Considering Figure 11, it may be observed that the pipe-to-soil potential (absolute values) varies at different points along the length of the pipeline parallel section. The computed values are higher at both ends of the pipeline (at the beginning and end of the pipeline) and zero at the midpoint of the pipeline length. Furthermore, in Figure 11, the option (i) of the transmission line phase conductors' transposition has the highest effect on the pipeline, in line with the result presented in Section 3.1. Pipelines installed near this condition of transmission lines has the highest pipe-to-soil potential. Considering the option (ii), the magnitude of the pipe-to-soil potential is very close for this condition. However, with a direct phase transposition of the transmission line phase conductors (option (iv)), there is a relatively large reduction in the computed values of pipe-to-soil potential along the length of the pipeline. A lower magnitude with a wider margin is observed with this option.

Moreover, the effect of these phase transpositions on the AC density through a 1 mm defect computed along the length of the pipeline is presented in Figure 12. In this figure, it may be observed that the result presented here follows the same pattern with that of Figure 11. The option (iv) of the phase conductors' transposition has the least AC density value with a wider margin than others. Moreover, such effect on the relative risk value of AC corrosion is presented in Figure 13. It may be observed that the result presented in this figure follows a similar pattern to those presented in Figure 11 and Figure 12.

4. CONCLUSION

In this paper, an assessment of the AC induced corrosion risk of a buried pipeline installed near an existing transmission line is presented. The assessment was demonstrated using a practical case of AC interference problem in one of the Rand Water sites, South Africa. The effects of the phase conductor transpositions of the transmission lines in the study site, soil resistivity and the steady-state current on the AC corrosion assessment indices are also presented. The results presented revealed that more attention should be given to pipelines installed in low resistivity environments to reduce the corrosion risk due to AC interference. Considering the effect of the energy demand on the AC corrosion rate, AC induced corrosion mitigation strategies and cathodic protection systems must be reviewed from time to time to meet the trend in energy demand. Furthermore, the effect of the transmission line phase conductors' arrangement cannot be overlooked and must be taken into consideration in designing an effective AC mitigation system.

ACKNOWLEDGMENT

This work was supported in part by the Tshwane University of Technology, Pretoria, South Africa, the Rand Water, South Africa.

REFERENCES

1. Ouadah, M., O. Touhami, and R. Ibtiouen, "Diagnosis of the AC current densities effect on the cathodic protection performance of the steel X70 for a buried pipeline due to electromagnetic interference caused by HVPTL," *Progress In Electromagnetics Research M*, Vol. 45, 163–171, 2016.
2. Ponnle, A. A., K. B. Adedeji, B. T. Abe, and A. A. Jimoh, "Variation in phase shift of multi-circuits HVTLs phase conductor arrangements on the induced voltage on buried pipeline: A theoretical study," *Progress In Electromagnetics Research B*, Vol. 69, 75–86, 2016.
3. Ponnle, A. A., K. B. Adedeji, B. T. Abe, and A. A. Jimoh, "Variation in phase shift of phase arrangements on magnetic field underneath overhead double-circuit HVTLs: Field distribution and polarization study," *Progress In Electromagnetics Research M*, Vol. 56, 157–167, 2017.
4. Cotton, I., C. Charalambous, P. Aylott, and P. Ernst, "Stray current control in DC mass transit systems," *IEEE Transactions on Vehicular Technology*, Vol. 54, No. 2, 722–730, 2005.

5. Ogunsola, A., A. Mariscotti, and L. Sandrolini, "Estimation of stray current from a DC-electrified railway and impressed potential on a buried pipe," *IEEE Transactions on Power Delivery*, Vol. 27, No. 4, 2238–2246, 2012.
6. Ouadah, M. H., O. Touhami, R. Ibtiouen, and M. Zergoug, "Method for diagnosis of the effect of AC on the X70 pipeline due to an inductive coupling caused by HVPL," *IET Science, Measurement & Technology*, Vol. 11, No. 6, 766–772, 2017.
7. Ouadah, M., O. Touhami, R. Ibtiouen, M. F. Benlamnouar, and M. Zergoug, "Corrosive effects of the electromagnetic induction caused by the high voltage power lines on buried X70 steel pipelines," *International Journal of Electrical Power & Energy Systems*, Vol. 91, 34–41, 2017.
8. Funk, D., W. Prinz, and H. Schoneich, "Investigations of AC corrosion in cathodically protected pipes," *Ochrona Przed Korozja*, Vol. 36, No. 10, 225–228, 1993.
9. Xu, L., X. Su, Z. Yin, Y. Tang, and Y. Cheng, "Development of a real-time AC/DC data acquisition technique for studies of AC corrosion of pipelines," *Corrosion Science*, Vol. 61, 215–223, 2012.
10. Jiang, Z., Y. Du, M. Lu, Y. Zhang, D. Tang, and L. Dong, "New findings on the factors accelerating AC corrosion of buried pipeline," *Corrosion Science*, Vol. 81, 1–10, 2014.
11. Christoforidis, G. C., D. P. Labridis, and P. S. Dokopoulos, "Inductive interference calculation on imperfect coated pipelines due to nearby faulted parallel transmission lines," *Electric Power Systems Research*, Vol. 66, 139–148, 2003.
12. Qi, L., H. Yuan, Y. Wu, and X. Cui, "Calculation of overvoltage on nearby underground metal pipeline due to the lightning strike on UHV AC transmission line tower," *Electric Power Systems Research*, Vol. 94, 54–63, 2013.
13. Bond, W. R., "The effect of overhead AC power line paralleling ductile iron pipelines," *Ductile Iron Pipe Research Association*, 1–8, Birmingham, 1997.
14. NACE RP0177, "Mitigation of alternating current and lightning effects on metallic structures and corrosion control systems," *NACE International Standard Practice*, Houston, Texas, 2007.
15. CEN/TS12954, "Cathodic protection of buried or immersed metallic structures: General principles and application for pipelines," *European Technical Specification*, Germany, 2001.
16. Schoneich, H. G., "Discussion of criteria to assess the alternating current corrosion risk of cathodically protected pipelines," *Proceedings of the 2004 CEOCOR Congress*, Dresden, Germany, Jun. 15–16, 2004.
17. Riegel, K., "Effect of cathodic protection levels and defect geometry on the AC corrosion on pipelines," *Proceedings of the CEOCOR Congress*, Malaga, Spain, May 9–11, 2007.
18. Buchler, M., C. Voute, and H. Schoneich, "The effect of variation of ac interference over time on the corrosion of cathodically protected pipelines," *Proceedings of the 2009 CEOCOR Congress*, 21–13, Vienna, Austria, May 26–29, 2009.
19. Micu, D. D., G. C. Christoforidis, and L. Czumbil, "AC interference on pipelines due to double circuit power lines: A detailed study," *Electric Power Systems Research*, Vol. 103, 1–8, 2013.
20. CEN/TS15280, "Evaluation of AC corrosion likelihood of buried pipelines-application to cathodically protected pipelines," *Technical Specification, CEN-European Committee for Standardization*, 2006.
21. Philip, S. D., "Overview of HVAC transmission line interference issues on buried pipelines," *Proceedings of the NACE Northern Area Western Conference*, Alberta, Canada, Feb. 15–18, 2010.
22. Nelson, J. P., "Power systems in close proximity to pipelines," *IEEE Transactions on Industry Applications*, Vol. 1A-22, No. 1, 435–441, 1986.
23. Djekidel, R. and D. Mahi, "Calculation and analysis of inductive coupling effects for HV transmission lines on aerial pipelines," *Przegld Elektrotechniczny*, Vol. 90, No. 9, 151–156, 2014.
24. Christoforidis, G. C., D. P. Labridis, and P. S. Dokopoulos, "A hybrid method for calculating the inductive interference caused by faulted power lines to nearby buried pipelines," *IEEE Transactions on Power Delivery*, Vol. 20, No. 2, 1465–1473, 2005.
25. Satsios, K. J., D. P. Labridis, and P. S. Dokopoulos, "Finite-element computation of field and eddy currents of a system consisting of a power transmission line above conductors buried in

nonhomogeneous earth," *IEEE Transactions on Power Delivery*, Vol. 13, No. 3, 876–882, 1998.

26. Popoli, A., A. Cristofolini, L. Sandrolini, B. T. Abe, and A. Jimoh, "Assessment of AC interference caused by transmission lines on buried metallic pipelines using FEM," *2017 ACES Symposium*, Florence, Italy, Mar. 26–30, 2017.
27. Carson, J. R., "Wave propagation in overhead wires with ground return," *Bell System Technical Journal*, Vol. 5, 539–554, 1926.
28. Pollaczek, F., "Sur le champ produit par un conducteur simple infiniment long parcouru par un courant alternatif," *Revue Gén, Elec.*, Vol. 29, 851–867, 1931.
29. Wedepohl, L. M. and D. J. Wilcox, "Transient analysis of underground power-transmission systems. System model and wave-propagation characteristics," *Proceedings of the IEE*, Vol. 120, No. 2, 253–260, 1971.
30. Lucca, G., "Mutual impedance between an overhead and a buried line with earth return," *Proceedings of the 9th IET International Conference on Electromagnetic Compatibility*, 80–86, Manchester, UK, Sep. 5–7, 1994.
31. Yoshihiro, B., A. Ametani, T. Yoneda, and N. Nagaoka, "An investigation of earth return impedance between overhead and underground conductors and its approximation," *IEEE Transactions on Electromagnetic Compatibility*, Vol. 5, No. 3, 860–867, 2009.
32. CIGRE, "Guide on the influence of high voltage AC power systems on metallic pipelines," *CIGRE Working Group 36.02 Technical Brochure*, No. 095, 1995.
33. Eskom, *Guideline on the Electrical Co-ordination of Pipeline and Power Lines*, Paper No. 240-66418968, 25–73, South Africa, 2015.
34. Lietai, Y., *Techniques for Corrosion Monitoring*, Wood Head Publishing Limited, Abington Hall, Abington, Cambridge CB21 6AH, England, 2008.
35. Dobrzanski, L. A., Z. Brytan, A. M. Grande, and M. Rosso, "Corrosion resistance of sintered duplex stainless steel evaluated by electrochemical method," *Journal of Achievements in Materials and Manufacturing Engineering*, Vol. 19, No. 1, 38–45, 2006.